International Journal For Technological Research In Engineering
Volume 9, Issue 11, July-2022 *ISSN (Online): 2347 - 4718*

BOUNDARY DISCRIMINATIVE NOISE DETECTION ALGORITHM IN SWITCHING MEDIAN FILTER

Dr. Ashish Joshi
Dept. of Electrical & Electronics Engineering
BM College of Technology, Indore

Abstract: - A novel, productive and straightforward motivation clamor finder for exchanging middle channel is proposed in this paper. The proposed technique thinks about the distinction worth of the ongoing pixel with the most brilliant and the haziest pixels in its functioning window and utilizations the distinction worth to decide if the ongoing pixel is ruined by drive commotion. To keep away from the phony problem produced in this first stage, the competitor pixels are passed however a subsequent stage utilizing nearby measurements. This new method can eliminate the indiscreet commotion from ruined pictures effectively and requires no past preparation and clamor measurements and strength for that reason. For execution assessment four motivation clamor models are thought of. Proposed calculation is oblivious to how much commotion. Quantitative and subjective examination, performed on standard dim scale pictures, demonstrate the way that proposed technique can identify drive commotion effectively under wide reach (up to 90%) of clamor thickness. The proposed strategy performs well as far as low miss and bogus identification and high PSNR esteem. In contrast with every single existing calculation, the proposed strategy performs well and outflanks the contenders for all the clamor models and for every one of the pictures. The addition is most unmistakable in the event of commotion model 3 and 4.

Index terms: Image denoising, Impulse noise, Impulse noise detection, switching median filter.

1. INTRODUCTION

During obtaining and transmission computerized pictures could be undermined by motivation (salt and pepper) clamor. Subsequently, some pixel values are unavoidably sullied while others remain commotion free. In picture handling, middle channel has been utilized for the expulsion of motivation commotion. Middle channel will in general alter both defiled and uncorrupted pixels, hence corrupts the performance of the separating. At the point when the pictures are profoundly undermined, countless drive pixels might associate into clamor blotches. In such cases, it is undeniably challenging to distinguish and wipe out the motivation commotion pixels. Likewise; the mistake will proliferate around their local areas.

Recently switching techniques have been applied for the removal of impulse noise. These techniques detect whether the current pixel is corrupted or uncorrupted and then filtering is applied only to those pixels which are found corrupted. Thus switching techniques give better performance in comparison to median filter. A large number of algorithms have been proposed to detect the impulse noise from corrupted images. These algorithms are based on mathematical morphology, image derivative, statistical approach and fuzzy techniques. As a detection scheme, morphological residue detector (MRD)[2] was proposed. MRD determine the impulse noise by comparing the difference between the value of the pixel and the result of opening and closing with a flat structuring element. Another method, Min-Max working window[3] was proposed. This method compares the current pixel with the maximum and minimum pixels in its working window. This method is easy to implement and requires no previous training. Fuzzy detec- tion method[5] is highly parameter dependent, requires adjustment of many parameters for the successful detection of noisy pixels. Another method, laplacian detector[6] was proposed based on the minimum absolute value of four convolutions obtained using one-dimensional laplacian operators. Adaptive switching median filter (ASMF)[7] calculates the noisy pixels using the vari- able sized detection window. Iterative adaptive switching median filter (IASMF)[10] is another promising technique. In this method identification of the corrupted pixels are performed using an iterative fixed sized smaller window. In progressive switching median filter (PSMF)[11] impulse detection procedure is applied through several iterations, which makes it difficult for real time implementation. Morphological adaptive switching median filter (MASMF)[12] uses two stage morphological noise detector to realize accurate noise detection. Boundary discriminative noise detection (BDND)[13] uses two stages, in which second stage will only be evoked conditionally. This method determines two boundaries for each pixel to classify whether it is corrupted or uncorrupted.

In this paper, inspired by BDND algorithm, an efficient impulse noise detector has been proposed. In the first stage both global and local characteristics of the noisy image are used. Use of global characteristics lowers the computational complexity. The second stage is fashioned in a different way for better performance. Proposed ABDND method can handle image corruption even up to 90% impulse noise density and shows better performance than all other existing techniques. As noise is of limited range within two boundaries, the uncorrupted pixels can be intelligently filtered out and could be used to estimate the corrupted pixels. It is a clue how the proposed algorithm can produce a good image even if there are more than 50% corrupted pixels. Furthermore, for the restoration of the corrupted image after detection of the noisy pixels, adaptive switching median filter is used for all

methods. Use of smaller window (11 × 11 instead of 21 × 21 in BDND) in first stage helps to speed up the algorithm.
The paper is divided into five sections. Section 2 describes the impulse noise models. Section 3 describes the proposed ABDND detection algorithm. Section 4 refers the noise adaptive filtering used for the restoration of corrupted images. Section 5 presents simulation results. Section 6 concludes this paper.

2. IMPULSE NOISE MODELS

For examining the performance of proposed detector four impulse noise models[13] are implemented assuming the corrupted pixels may have values equal to or near the maximum and minimum of the allowable dynamic range. For each original image pixel at location (i, j) the intensity value is si,j , the corresponding pixel of the noisy image is given by xi,j. Probability density function of each impulse noise model is as follows.

2.1 Noise Model 1

Here corrupted image have fixed value for salt (i.e. 255) and pepper (i.e. 0) noise with equal probability, the probability distribution function is given by:

$$f(x) = \begin{cases} \frac{p}{2} & \text{for } x = 0 \\ 1-p & \text{for } x = s_{i,j} \\ \frac{p}{2} & \text{for } x = 255 \end{cases}$$

where p is the noise density in the image.

2.2 Noise Model 2

Here corrupted image have fixed value for salt (i.e. 255) and pepper (i.e. 0) noise with unequal probability, the probability distribution function is given by:

$$f(x) = \begin{cases} p_1 & \text{for } x = 0 \\ 1-p & \text{for } x = s_{i,j} \\ p_2 & \text{for } x = 255 \end{cases}$$

where p = p1 + p2 is the noise density in the image and p1 /= p2.

2.3 Noise Model 3

Here corrupted image have dynamic values for salt (i.e. 255-m to 255) and pepper (i.e. 0 to m) noise with equal probability, the probability distribution function is given by:

$$f(x) = \begin{cases} \frac{p}{2m} & \text{for } 0 \le x \le m \\ 1-p & \text{for } x = s_{i,j} \\ \frac{p}{2m} & \text{for } 255-m \le x \le 255 \end{cases}$$

where p is the noise density in the image.

2.4 Noise Model 4

Here corrupted image have dynamic values for salt (i.e. 255-m to 255) and pepper (i.e. 0 to m) noise with unequal probability, the probability distribution function is given by:

$$f(x) = \begin{cases} \frac{p_1}{m} & \text{for } 0 \le x \le m \\ 1-p & \text{for x=}s_{i,j} \\ \frac{p_2}{m} & \text{for } 255-m \le x \le 255 \end{cases}$$

for $255 - m \le x \le 255$

where p = p1 + p2 is the noise density in the image and p1 /= p2.

3. IMPULSE NOISE DETECTION

Here an advanced boundary discriminative noise detection (ABDND) algorithm is proposed, which can handle impulse noise up to 90% noise density. Proposed algorithm is very simple and easy to implement.
Propose algorithm consists of two stages. In the first stage all pixels examined to prepare a first stage noise map, which keeps the location information of noisy pixels. This stage makes use of global as well as local statistics of the image. In the second stage only those pixels marked noisy in first stage are examined using local statistics to confirm whether they are corrupted. In the second stage the first stage noise map is modified accordingly to get final noise map. In the final noise map '1' and '0' values signify the location of corrupted pixel and uncorrupted pixel
respectively.

Steps of proposed ABDND algorithm for 8-bit images are as follows:
Step1 : Obtain the histogram of the noisy image.
Step2 : Calculate the forward difference between the adjacent histogram counts in histogram array and obtain a difference array (Dif f),

$$Diff_i = Hist_{i+1} - Hist_i for \quad i \in [0, 254$$

where Histi is the histogram count at ith index (indicating gray scale value) and Diffi is the forward difference at ith index. Histogram of original 'Lenna' image, noisy 'Lenna' image corrupted with noise model 4 (50% noise density) and plot of histogram forward difference Diff is shown in Fig.1.
Step3 : Forward difference array Dif f have positive and negative maximum. Set T1 = index corresponding to negative maximum in difference array
T2 = 256 - (index corresponding to positive maximum in difference array)
(Here, the underlying assumption is the image histogram is smooth and due to addition of impulsive noise, two jumps are introduced in the corrupted image histogram. The estimates T1 and T2 signify the location of impulsive noise.)
According to Fig.1 negative maximum and positive maximum occur at index value 10 and 246 respectively in difference array thus T1 = 10 and T2 = 256 — 246 = 10.

Step4 : For each pixel in noisy image impose a 11 × 11 window, which is centered on the current pixel, and find out the maximum value (smax) and minimum value (smin) within the window. In this stage the pixels are very conservatively labeled as uncorrupted.
Use the following equation and prepare a first stage noise map r.

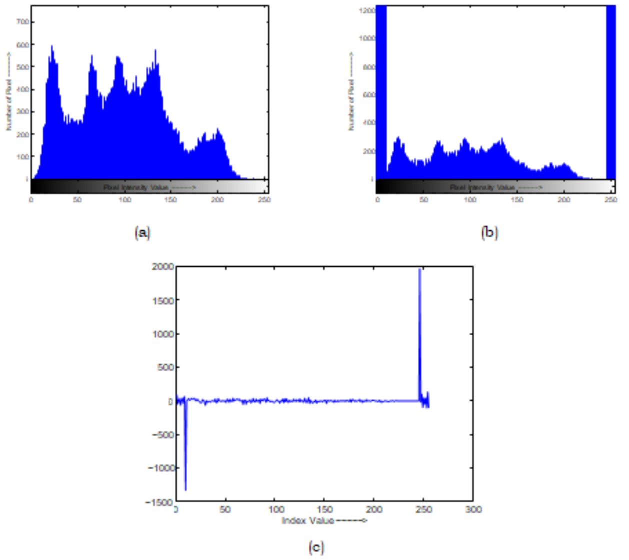

Figure 1: (a) Histogram of original ‘Lenna’ image, (b) Histogram of noisy ‘Lenna’ image corrupted with 50% impulse noise according to noise model 4, (c) Plot of Vector Dif f .

corresponding pixel in noisy image is uncorrupted.
Step5 : For each corrupted pixel in image (having corresponding value ‘1’ in first stage noise map) following actions are performed:
Level 1 : Impose a w × w window around the noisy pixel in noisy image, such that w is much smaller than previous window size (i.e. 11). If more than w uncorrupted pixels (i.e. pixels which have corresponding values in first stage noise map ‘0’) are found, then calculate the sum of the absolute difference between the uncorrupted pixels and the central noisy pixel and go to Level 3 else go to Level 2.
Level 2 : Set the w = w + 2 and go to Level 1. Increase the window up to a pre determined fixed size.
Level 3 : The minimum of the difference of intensity value of the central noisy pixel from

both end (i.e. 0 and 255) is taken as T_3. Therefore,

$$T_3 = min(s_{i,j} - 0, \quad 255 - s_{i,j})$$

If sum of the absolute difference between the uncorrupted pixels and the central noisy pixel is less than the threshold T3, mark the corresponding pixel as uncorrupted (in first stage noise map r reset the corresponding location to 0) else leave it unchanged. In other words, if the pixel under consideration is found near the uncorrupted pixels is marked as uncorrupted. Then proceed to next noisy pixel and start from Level 1.
Example : Let us consider the pixel ⟨10⟩ which is detected as noisy pixel in the first stage (Step 5). The local 3 × 3 window around that pixel and corresponding noise map are given as

$$\begin{pmatrix} 0 & 8 & 11 \\ 248 & \langle 10 \rangle & 2 \\ 11 & 9 & 249 \end{pmatrix} \quad and \quad \begin{pmatrix} 1 & 0 & 0 \\ 1 & \langle 1 \rangle & 1 \\ 0 & 0 & 1 \end{pmatrix}$$

The uncorrupted pixels within this window are (8, 11, 11, 9) respectively. As there are 4 uncorrupted pixels which is greater than the window dimension 3, compute the absolute difference of uncorrupted pixels with respect to the central pixel as {|8 — 10|, |11 — 10|, |11 — 10|, |9 — 10|} or {2, 1, 1, 1}. The corresponding sum of absolute difference is = (2 + 1 + 1 + 1)=5. Then compare this sum of absolute difference to the threshold T3 = min[(10 — 0), (255 — 10)] = 10. Since 5 < 10, the central pixel ⟨10⟩ is detected as uncorrupted and hence the corresponding location in first stage noise map is reset to ‘0’.
Now this noise map r is called as final noise map. This final noise map has values 0 and 1, where 0 and 1 denote the corresponding pixel is uncorrupted and corrupted respectively.

4. NOISE ADAPTIVE FILTERING

After noise detection adaptive switching median filter (ASMF)[7] is used with ABDND algorithm for image restoration. ASMF gives acceptable result at lower noise density, while produces comparable results at higher noise density. Other median filters develop many impulse patches at 60% or higher noise levels, while ASMF generates a recognizable and patch free restoration.
Table 1: Numbers of miss detection (MD) and false detection (FD) values resulting by vari- ous noise detection algorithms on ‘Lenna’ image with noise density varying from 10% to 90% distributed according to noise model 1.

Method		Noise Density(%)								
		10	20	30	40	50	60	70	80	90
MRD	MD	0	0	0	0	0	0	0	0	0
	FD	13	1	0	0	0	0	0	0	0
Min-Max	MD	0	0	0	0	0	0	0	0	0
	FD	10	1	0	0	0	0	0	0	0
Fuzzy	MD	0	0	0	4	11	34	69	110	197
	FD	2854	2485	1912	1317	765	518	272	133	72
Laplacian	MD	126	557	1413	2697	4107	6311	8860	11192	13394
	FD	431	741	1279	1940	2391	2595	2348	1923	1089
ASMF	MD	0	0	0	0	0	0	0	0	0
	FD	14	0	0	0	0	0	0	0	0
IASMF	MD	0	0	0	0	0	0	0	0	0
	FD	10	14	30	41	35	66	65	55	48
PSMF	MD	487	882	1394	1862	2323	2921	3756	6754	15851
	FD	1873	1814	1774	1841	1876	2239	2907	3530	3442
MASMF	MD	0	0	0	0	0	0	0	0	0
	FD	231	21	0	0	0	0	0	0	0
BDND	MD	0	0	0	0	0	0	0	0	0
	FD	7	4	4	5	8	6	7	9	65
ABDND	MD	0	0	0	0	0	0	0	0	0
	FD	10	1	0	0	0	0	0	0	0

Table 2: PSNR values resulting by various noise detection algorithms on ‘Lenna’ image with noise density varying from 10% to 90% distributed according to noise model 1.

Method	Noise Density(%)								
	10	20	30	40	50	60	70	80	90
MRD	**38.92**	**34.69**	**32.60**	**30.63**	**28.98**	**27.50**	**26.18**	**24.66**	**22.47**
Min-Max	**38.92**	**34.69**	**32.60**	**30.63**	**28.98**	**27.50**	**26.18**	**24.66**	**22.47**
Fuzzy	33.98	32.66	31.21	29.84	28.12	26.65	24.58	21.50	18.16
Laplacian	32.95	31.56	26.20	21.39	17.64	15.44	11.47	8.01	6.60
ASMF	**38.92**	**34.69**	**32.60**	**30.63**	**28.98**	**27.50**	**26.18**	**24.66**	**22.47**
IASMF	**38.92**	**34.69**	32.59	30.62	28.97	27.48	26.17	24.63	22.41
PSMF	27.89	27.37	26.34	25.66	23.95	20.89	15.83	10.62	6.92
MASMF	38.35	**34.69**	**32.60**	**30.63**	**28.98**	**27.50**	**26.18**	**24.66**	**22.47**
BDND	**38.92**	**34.69**	**32.60**	**30.63**	**28.98**	**27.50**	**26.18**	**24.66**	22.28
ABDND	**38.92**	**34.69**	**32.60**	**30.63**	**28.98**	**27.50**	**26.18**	**24.66**	**22.47**

5. SIMULATION RESULTS

To verify the performances of various noise detection algorithms, simulations are carried out on the well-known 8-bit gray scale images ('Lenna', and 'Baboon') in MATLAB 7.0.4 environment

Table 3: Numbers of miss detection (MD) and false detection (FD) values resulting by vari- ous noise detection algorithms on 'Lenna' image with noise density varying from 10% to 90% distributed according to noise model 2.

Method		Noise Density(%)								
		10 (6+4)	20 (8+12)	30 (20+10)	40 (25+15)	50 (20+30)	60 (25+35)	70 (40+30)	80 (35+45)	90 (40+50)
MRD	MD	0	0	0	0	0	0	0	0	0
	FD	84	0	0	0	0	0	0	0	0
Min-Max	MD	0	0	0	0	0	0	0	0	0
	FD	19	0	0	0	0	0	0	0	0
Fuzzy	MD	0	0	6	10	23	57	114	171	294
	FD	2971	2590	2235	1485	945	558	305	170	64
Laplacian	MD	141	598	1982	3411	4873	7168	9650	12293	14210
	FD	501	817	1715	2195	2747	2956	2464	1957	1234
ASMF	MD	0	0	0	0	0	0	0	0	0
	FD	18	0	0	0	0	0	0	0	0
IASMF	MD	0	0	0	0	0	0	0	0	0
	FD	13	16	45	67	85	91	82	84	56
PSMF	MD	589	712	1999	2744	1601	2243	6415	9747	19329
	FD	1859	1834	2001	2016	2314	2887	3526	4749	4003
MASMF	MD	0	0	0	0	0	0	0	0	0
	FD	220	38	11	1	0	0	0	0	0
BDND	MD	0	0	0	0	0	0	0	0	0
	FD	3	3	6	15	7	10	16	66	618
ABDND	MD	0	0	0	0	0	0	0	0	0
	FD	18	1	0	0	0	0	0	0	0

Table 4: PSNR values resulting by various noise detection algorithms on 'Lenna' image with noise density varying from 10% to 90% distributed according to noise model 2.

Method	Noise Density(%)								
	10 (6+4)	20 (8+12)	30 (20+10)	40 (25+15)	50 (20+30)	60 (25+35)	70 (40+30)	80 (35+45)	90 (40+50)
MRD	38.91	**34.84**	**32.78**	**30.19**	**28.80**	**27.81**	**25.99**	**24.48**	**22.49**
Min-Max	**38.92**	**34.84**	**32.78**	**30.19**	**28.80**	**27.81**	**25.99**	**24.48**	**22.49**
Fuzzy	33.70	32.67	30.72	29.19	27.99	25.55	23.17	21.60	17.62
Laplacian	30.91	24.81	18.51	15.41	13.48	11.35	9.25	7.89	6.61
ASMF	**38.92**	**34.84**	**32.78**	**30.19**	**28.80**	**27.81**	**25.99**	**24.48**	**22.49**
IASMF	**38.92**	**34.84**	32.72	30.18	28.79	27.76	25.97	24.46	22.17
PSMF	28.01	27.33	25.83	24.58	23.60	19.41	13.63	9.53	6.40
MASMF	37.47	34.12	31.61	30.19	28.80	27.81	25.98	24.48	22.49
BDND	**38.92**	**34.84**	**32.78**	**30.19**	**28.80**	**27.81**	**25.99**	**24.48**	22.48
ABDND	**38.92**	**34.84**	**32.78**	**30.19**	**28.80**	**27.81**	**25.99**	**24.48**	**22.49**

Table 5: Numbers of miss detection (MD) and false detection (FD) values resulting by vari- ous noise detection algorithms on 'Lenna' image with noise density varying from 10% to 90% distributed according to noise model 3.

Method		Noise Density(%)								
		10	20	30	40	50	60	70	80	90
MRD	MD	1785	7598	13800	20206	25907	32344	38692	42932	44932
	FD	1102	50	4	0	0	0	0	0	0
Min-Max	MD	1085	3885	7499	12246	17368	23058	28735	34785	40689
	FD	3316	2790	2092	1297	896	447	254	129	51
Fuzzy	MD	120	813	2264	4782	7931	11848	16539	21536	27194
	FD	10017	10171	8521	6342	4552	3038	1953	1164	506
Laplacian	MD	170	692	1385	2586	4241	6244	8574	10719	12828
	FD	534	873	1537	2170	2771	2803	2712	2175	1266
ASMF	MD	4255	10144	15791	21325	27234	32775	38710	44010	49573
	FD	19	0	0	0	0	0	0	0	0
IASMF	MD	5840	11657	17300	23248	29053	34984	40448	46270	50223
	FD	3	0	0	0	0	0	0	0	0
PSMF	MD	530	1054	1527	2058	2662	3221	4360	7410	16779
	FD	1890	1892	1787	1753	1800	2134	2897	3604	3312
MASMF	MD	3726	9615	15911	22083	27963	33991	40036	46411	52401
	FD	229	27	2	0	0	0	0	0	0
BDND	MD	0	38	192	712	1859	3670	6762	10431	15975
	FD	7	7	7	23	21	12	36	41	109
ABDND	MD	0	0	0	0	0	0	0	0	0
	FD	270	134	103	93	66	55	45	30	15

Table 6: PSNR values resulting by various noise detection algorithms on 'Lenna' image with noise density varying from 10% to 90% distributed according to noise model 3

Method	Noise Density(%)								
	10	20	30	40	50	60	70	80	90
MRD	20.43	14.49	11.91	10.30	9.12	8.14	7.39	6.78	6.20
Min-Max	21.59	15.90	13.07	11.06	9.62	8.45	7.58	6.83	6.22
Fuzzy	27.27	20.81	16.63	13.78	11.52	9.65	8.40	7.30	6.41
Laplacian	32.29	27.54	22.99	19.51	16.49	13.83	11.27	9.41	7.60
ASMF	16.78	13.01	11.10	9.69	8.66	7.73	7.08	6.42	5.89
IASMF	15.94	12.88	11.15	9.89	8.87	8.02	7.28	6.67	6.02
PSMF	28.01	27.51	26.60	25.53	24.87	22.31	18.37	11.98	7.33
MASMF	17.71	13.64	11.47	10.07	9.06	8.10	7.39	6.76	6.21
BDND	**37.52**	33.97	29.52	26.01	25.66	22.61	18.22	11.99	8.63
ABDND	37.49	**34.03**	**31.85**	**30.25**	**28.57**	**27.21**	**25.99**	**24.01**	**21.79**

Table 7: Numbers of miss detection (MD) and false detection (FD) values resulting by vari- ous noise detection algorithms on 'Lenna' image with noise density varying from 10% to 90% distributed according to noise model 4.

Method		Noise Density(%)								
		10 (6+4)	20 (8+12)	30 (20+10)	40 (25+15)	50 (20+30)	60 (25+35)	70 (40+30)	80 (35+45)	90 (40+50)
MRD	MD	1779	7027	13676	19914	26504	32504	38601	44762	50254
	FD	1238	67	22	0	0	0	0	0	0
Min-Max	MD	1107	3862	7764	12613	17740	23220	28698	34704	40795
	FD	3271	2948	2449	1634	1016	631	362	153	66
Fuzzy	MD	138	904	2732	5177	7930	11411	16565	21090	27115
	FD	10048	10253	8880	6745	4981	3396	2138	1212	501
Laplacian	MD	205	616	2019	3189	4632	6776	9414	11594	14339
	FD	554	980	1906	2454	3165	3271	2819	2301	1305
ASMF	MD	4362	10134	15920	21417	27289	32780	38492	44095	49588
	FD	19	0	0	0	0	0	0	0	0
IASMF	MD	5765	11497	17281	23150	28790	34798	40632	50992	52343
	FD	0	0	0	0	0	0	0	0	0
PSMF	MD	667	810	2283	2861	1831	2468	6932	10050	19681
	FD	1855	1903	1968	2027	2339	2822	3450	4706	3859
MASMF	MD	226	23	12	2	1	0	0	0	0
	FD	4079	9753	15825	21965	27988	34189	40665	46278	52342
BDND	MD	0	35	385	1047	2283	4220	7015	11511	23317
	FD	7	14	30	27	25	21	49	142	562
ABDND	MD	0	0	0	0	0	0	0	0	0
	FD	288	149	109	86	72	55	41	30	18

Table 8: PSNR values resulting by various noise detection algorithms on 'Lenna' image with noise density varying from 10% to 90% distributed according to noise model 4.

Method	Noise Density(%)								
	10 (6+4)	20 (8+12)	30 (20+10)	40 (25+15)	50 (20+30)	60 (25+35)	70 (40+30)	80 (35+45)	90 (40+50)
MRD	20.18	14.29	12.02	10.38	9.08	8.16	7.45	6.77	6.18
Min-Max	21.05	15.93	12.92	11.11	9.52	8.45	7.63	6.80	6.21
Fuzzy	26.59	20.32	16.07	13.61	11.17	9.48	8.48	7.21	6.39
Laplacian	31.78	27.78	21.81	18.19	15.48	13.29	11.06	8.94	7.41
ASMF	17.24	12.68	11.70	10.15	8.27	7.48	7.33	6.21	5.74
IASMF	16.23	12.56	11.71	10.26	8.55	7.72	7.54	6.39	5.85
PSMF	27.69	27.15	26.17	25.03	23.41	20.29	15.65	10.42	6.98
MASMF	17.80	13.60	11.55	10.10	8.89	8.03	7.42	6.71	6.18
BDND	**37.39**	34.30	27.38	26.11	23.40	20.11	15.48	11.40	7.42
ABDND	37.33	**34.31**	**32.17**	**30.28**	**28.71**	**27.15**	**25.86**	**24.23**	**21.81**

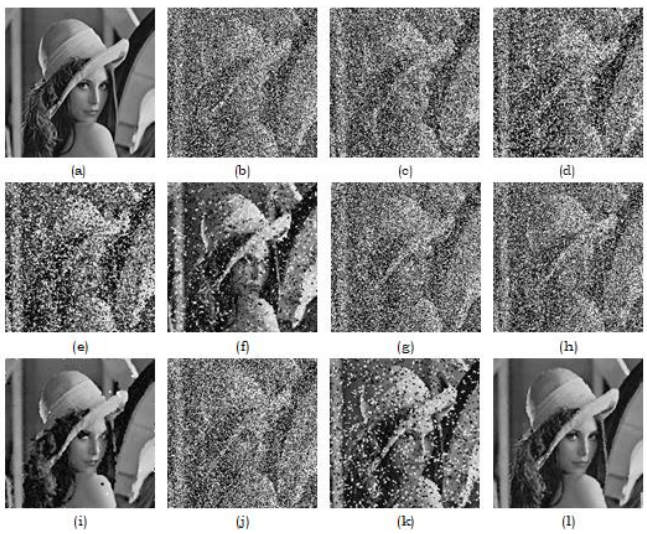

Figure 2: (a) original 'Lenna' image, (b) corrupted with 60% impulse noise according to noise model 3, restored by (c) MRD, (d) Min-Max, (e) Fuzzy, (f) Laplacian, (g) ASMF, (h) IASMF,
(i) PSMF, (j) MASMF, (k) BDND, (l) Proposed (ABDND) detection algorithm followed by adaptive switching median filter.

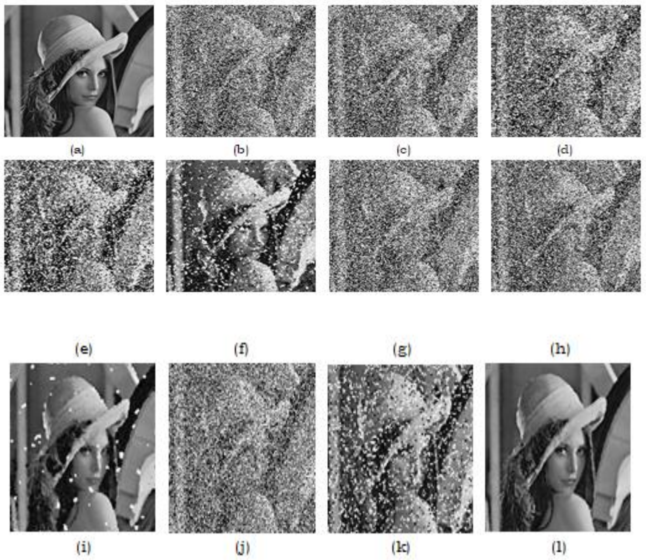

Figure 3: (a) original ‘Lenna’ image, (b) corrupted with 60% impulse noise according to noise model 4, restored by (c) MRD, (d) Min-Max, (e) Fuzzy, (f) Laplacian, (g) ASMF, (h) IASMF,
(i) PSMF, (j) MASMF, (k) BDND, (l) Proposed (ABDND) detection algorithm followed by adaptive switching median filter.

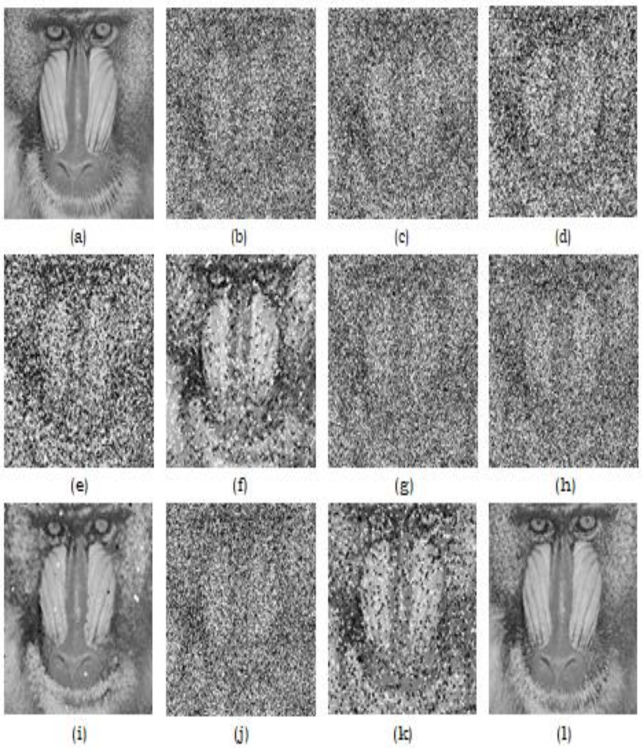

Figure 4: (a) original ‘Baboon’ image, (b) corrupted with 60% impulse noise according to noise model 3, restored by (c) MRD, (d) Min-Max, (e) Fuzzy, (f) Laplacian, (g) ASMF, (h) IASMF,
(i) PSMF, (j) MASMF, (k) BDND, (l) Proposed (ABDND) detection algorithm followed by adaptive switching median filter.

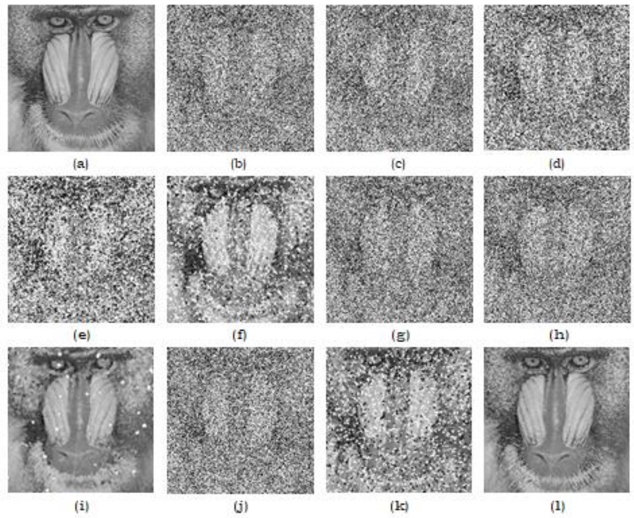

Figure 5: (a) original ‘Baboon’ image, (b) corrupted with 60% impulse noise according to noise model 4, restored by (c) MRD, (d) Min-Max, (e) Fuzzy, (f) Laplacian, (g) ASMF, (h) IASMF,
(i) PSMF, (j) MASMF, (k) BDND, (l) Proposed (ABDND) detection algorithm followed by adaptive switching median filter.

with noise densities varying from 10% to 90% for the all four impulse noise models[13]. For the impulse noise model 3 and 4 value of m is set to 10. For the comparison MRD, Min-Max, Fuzzy, Laplacian, ASMF, IASMF, PSMF, MASMF and BDND noise detection techniques are selected for the simulation experiment based on their merits. For the proposed algorithm value of w (Level 1 of Step 5) is 3 and window size is increased up to w = 15 (Level 1 of Step 5)
i.e. pre determined size of maximum window is 15. These values are experimentally derived considering different 8 bit images corrupted with all the four noise models with all possible noise densities. As small window value captures the local property better and keeps the computation under control, the minimum square window of 3 × 3 is chosen as starting point. Simulating under various noise conditions and on various gray scale images, it is found that the maximum window size 15 is sufficient and in the simulation experiment the algorithm never touched this limit. These minimum and maximum window sizes are fixed and set before the experiment. These values remains unchanged for all the noise densities, noise models and all the images used for simulation. It means the proposed ABDND algorithm is data agnostic. For restoration of corrupted image we employ adaptive switching median filter[7] for all detection methods.

5.1 Quantitative Performance

To evaluate the quantitative performance of the ABDND algorithm, the measure of miss detection and false detection are adopted. Since the noise detection plays the key role on filtering, it would be insightful to evaluate the performance of the noise detection algorithm at the first place. Miss detection means that a noisy pixel is detected as an uncorrupted pixel. False detection means that an uncorrupted pixel is detected as a noisy pixel[18]. Thus, as the miss-detection value and/or false-detection increases, the performance of the detector

decreases. Performance of restoration is evaluated by Peak-Signal-to-Noise Ratio (PSNR).
For the 8-bit restored image Z of size M × N , the PSNR is

$$PSNR = 10\log_{10}\frac{(255)^2}{MSE} \quad dB$$

where mean square error (MSE) is

$$MSE = \frac{\sum_{i=1}^{M}\sum_{i=1}^{M}(Z(i,j) - A(i,j))^2}{M \times N}$$

with respect to the noise free original image A.

Results shown for all detection algorithms are obtained on best possible value of the dependent parameters. For MRD, window size 13 for noise model 1 and 2 and 11 for noise model 3 and 4 give the best result. For Min-Max algorithm window size 9 and T=30 for noise model 1 and 2 and window size 3 and T=30 for noise model 3 and 4 are optimal. For fuzzy detector w1 = 30, w2 = 10 and u = 1 for noise model 1 and 2 and for noise model 3 and 4, w1 = 20, w2 = 25 and u = 2 gives the best result. For best result Laplacian detector threshold value should be 140 and 130 for noise model 1 and 2 and for noise model 3 and 4 respectively. For PSMF threshold value is 35 for all noise models and ASMF, IASMF and BDND detection algorithms are threshold independent. For MASMF algorithm threshold is 25 and window size is 7. For proposed ABDND algorithm there is no parameter to be adjusted.
For the 'Lenna' image the miss and false detection results are given in Table 1, 3, 5 and 7 for the four noise models described in section 2. The corresponding PSNR values are given in Table 2, 4, 6 and 8 respectively.
Morphological residue detector gives zero miss detection and small amount of false detection at all the noise densities for impulse noise model 1 and 2, but for impulse model 3 and 4, at all noise densities false detection is very low and miss detection is very large. Min-Max window detector for impulse noise model 1 and 2 gives zero miss and false detection but for impulse noise model 3 and 4, miss detection is very large. Fuzzy detector gives low miss detection and significant amount of false detection at all the noise densities for impulse noise model 1 and 2, but for impulse model 3 and 4, at all noise densities both miss and false detection are very large. For laplacian detector, for all impulse noise models miss and false detection increases as the noise density increases. ASMF gives almost zero miss and false detection for impulse noise model 1 and 2 but for impulse noise model 3 and 4 miss detection is very large. Performance of IASMF is similar to ASMF. For PSMF as the noise density increases miss and false detection increases for all impulse noise models. MASMF performs well for impulse noise model 1 and 2 but for impulse noise model 3 and 4 miss detection is large. BDND performs good for impulse noise model 1 and 2 by giving almost zero miss and very low false detection and for impulse noise model 3 and 4, it gives good result at low noise density but performance degrade at high noise density. Proposed ABDND method performs well for all impulse noise models. It achieves almost zero miss detection and low false detection at all noise density and accurate noise detection results as a higher PSNR value. While the performance gain of the proposed method is marginal in model 1 and 2, the performance gain is evident for the model 3 and 4, specially for high noise condition. It is interesting to note that for ABDND there is small false detections and no miss detections at the lowest noise density for all the noise models, however the false detections decrease with increase in noise density without any appreciable change in miss detection pattern. This can be explained by observing the value of the threshold T3. By setting a high value for T3, the false detection will decrease but the miss detection may increase. Hence, the threshold T3 should be chosen carefully for optimal result. In the proposed ABDND algorithm the threshold T3 is made data driven to work for all images corrupted with any of the four noise models at any noise density up to 90%. By manual selection of T3 the performance of the ABDND can be further improved for a particular situation. Here it may be also noted that due to these false detections, the PSNR result is affected only at the 2nd order place of decimal point.

5.2 Qualitative Performance

Qualitative performances of all detection algorithms are evaluated on standard 8 bit gray scale images. For that purpose the 60% impulse noise condition on 'Lenna', and 'Baboon' images are presented for impulse noise model 3 and 4 in Fig. 2, Fig. 3, Fig. 4 and Fig. 5. For the restoration of the image, all detection algorithms are followed by the adaptive switching median filter. For all the cases the proposed method gives the best result followed by PSMF and BDND algorithm. While the difference is small for model 1 and 2, the improvement is very clear for model 3 and 4 for all the images.

5.3 Complexity of the algorithm

Complexity of the Proposed algorithm is compared with the BDND algorithm at the 90% impulse noise. For an N × M image, average computational complexity for the BDND algorithm are approximately 1337NM . For the same image average computational complexity for the proposed ABDND algorithm are 599NM + 765. Hence for an 256 × 256 image computational complexity of the proposed algorithm are 0.45 times the BDND algorithm.

6. CONCLUSION

In this paper, a novel, exact and straightforward drive commotion recognition technique is proposed. The proposed clamor recognition calculation is of two phase. The main stage utilizes worldwide and nearby picture measurements to make it quick. The following stage assists with disposing of the misleading discoveries, bringing about the exhibition near the best exchanging middle channel. The calculation is totally information driven as in it doesn't need to remotely set any boundary. To reproduce the genuine condition, four commotion models are utilized. Broad recreations results uncover that proposed ABDND identification calculation outflanks the other existing recognition calculations by accomplishing zero miss discovery and extremely low bogus location for all commotion densities (up to 90%). Proposed location calculation followed by exchanging channel could be a strong plan for picture separating on the grounds that it accomplishes higher PSNR for all clamor densities. The presentation contrast with the contenders is more obvious for clamor model 3 and 4, where drive commotion is spread over a reach. It very well may be effectively infer that progress of such execution in light of the exact commotion identification plot. The two phases technique is intended to hold the calculation to the base for ongoing utilization of the proposed strategy.

REFERENCES

[1] Jain,A.K.: ‘Fundamentals of Digital Image Processing’, Prentice Hall of India, First Edition, 1989.

[2] Ze-Fang,D., Zhou-Ping,Y., and You-Lou,X.: ‘High Probability Impulse Noise Removing Al- gorithm Based on Mathematical Morphology’, IEEE Signal Processing Letters, 2007, 14, (1).

[3] Chen,P.Y., Lien,C.Y., and Tsai,C.Y.: ‘An Effective Impulse Noise Detector of Switching Median Filter using Min-Max Working Window’, Proc. of IEEE International Conference on Intelligent Information Hiding and Multimedia Signal Processing, 2007.

[4] Pok,G., Liu,J.C., and Nair,A.S.: ‘Selective removal of impulse noise based on homogeneity level information’, IEEE Trans. Image Processing’, 2003, 12, (1), pp. 85-92.

[5] Luo,W.: ‘An efficient algorithm for the removal of impulse noise from corrupted images’, Int. J. Electron. Commun. (AEU), 2006, 61, pp. 551-555.

[6] Zhang,S., and Karim,M.A.: ‘A New Impulse Detector for Switching Median Filter, IEEE Signal Processing Letters’, 2002, 9, (11).

[7] Nallaperumal,K., Varghese,J., and Saudia,S.: ‘Salt & Pepper Impulse Noise Removal using Adaptive Switching Median Filter’, Proc. of IEEE Oceans, Asia Pacific, Singapore, 2006.

[8] Garnett,R., Huegerich,T., Chui,C., and He,W.: ‘A universal noise removal algorithm with an impulse detector’, IEEE Trans. Image Processing, 2005, 14, (11), pp. 1747-54.

[9] Xu,X., Miller,E.L., Chen,D., and Sarhadi,M.: ‘Adaptive two-pass rank order filter to remove impulse noise in highly corrupted images’, IEEE Trans. Image Processing, 2004, 13, (2).

[10] Nallaperumal,K., Varghese,J., and Saudia,S.: ‘Iterative Adaptive Switching Median Filter’, proc. of IEEE ICIEA , Singapore, 2006.

[11] Wang,Z., and Zhang,D.: ‘Progressive switching median filter for removal of impulse noise from highly corrupted images’, IEEE Trans. Circuits and Systems-II: Analog and Digital Signal Processing, 1999, 46, (1).

[12] Zhang,X., Yin,Z., and Xiong,Y.: ‘Adaptive switching mean filter for impulse noise’, Congress on image and signal processing, CISP, 2008, 3, pp. 275-278.

[13] Ng,P.E., and Ma,K.K.: ‘A Switching Median Filter with Boundary Discriminative Noise Detection for Extremely Corrupted Images’, IEEE Transactions on Image Processing, 2006, 15, (6).

[14] Eng,H.L., and Ma,K.K.: ‘Noise Adaptive Soft-Switching Median Filter’, IEEE Transactions on Image Processing, 2001, 10, (2).

[15] Abreu,E., Lightstone,M., Mitra,S.K., and Arakawa,K.: ‘A new efficient approach for the re- moval of impulse noise from highly corrupted images’, IEEE Transactions on Image Process- ing, 1996, 5, (6).

[16] Hwang,H., and Haddad,R.: ‘Adaptive median filters: New algorithms and results’, IEEE Transactions on Image Processing, 1995, 4, (4), pp. 499-502.

[17] Ko,S.J., and Lee,Y.H.: ‘Center weighted median filters and their applications to image enhancement’, IEEE Trans. Circuits Syst. Video Technol., 1991, 38, pp. 984-993.

[18] Duda,R.O., Hart,P.E., and Stork,D.G.: ‘Pattern Classification’, John Wiley & Sons, Second Edition, 2001.

